

Supplementary Information for

## Designer aromatic peptide amphiphiles for self-assembly and enzymatic display of proteins with morphology control

Rie Wakabayashi,<sup>\*a</sup> Ayumi Suehiro,<sup>a</sup> Masahiro Goto,<sup>ab</sup> and Noriho Kamiya<sup>\*ab</sup>

[a] *Department of Applied Chemistry, Graduate School of Engineering, Kyushu University, 744 Motoooka, Nishi-ku, Fukuoka 819-0395, Japan.*

[b] *Center for Future Chemistry, Kyushu University, 744 Motoooka, Nishi-ku, Fukuoka 819-0395, Japan.*

E-mail: rie\_wakaba@mail.cstm.kyushu-u.ac.jp (R.W.)

kamiya.noriho.367@m.kyushu-u.ac.jp (N.K.)

### Table of Contents

1. Materials and methods	S2
2. Characterization of Fmoc-LnQG peptides	S5
3. Critical aggregation concentration determination of Fmoc-LnQG peptides	S5
4. Confocal fluorescence microscope images of Fmoc-LnQG peptide assemblies	S6
5. Conjugation of Fmoc-LnQG and fluorescein cadaverine (FC) by MTG catalysis	S6
6. Confocal fluorescence microscope images of FC on Fmoc-LnQG peptide assemblies	S8
7. Reaction kinetics of MTG-catalyzed reaction of Fmoc-LnQG	S9
8. Difference in the reaction kinetics by MTG between Fmoc-L <sub>2</sub> QG and Fmoc-L <sub>3</sub> QG	S10
9. Sequence of proteins used in this study	S10
10. Time-course of conjugation of Fmoc-LnQG with CK-EGFP by MTG	S11
11. Fluorescence properties of CK-EGFP before and after MTG reaction	S12
12. Influence of MTG reaction on Fmoc-LnQG peptide assemblies	S13
13. Influence of MTG reaction on CK-EGFP display on Fmoc-LnQG peptide assemblies	S15
14. Conjugation of CK-EGFP on Fmoc-LnQG by MTG catalysis	S16

## 1. Materials and methods

**Materials.** H-Gly-Trt(2-Cl)-resin, Fmoc-Leu-OH, Fmoc-Gln(Trt)-OH, *O*-(1H-benzotriazol-1-yl)-*N,N,N',N'*-tetramethyluronium hexafluorophosphate (HBTU), 1-hydroxy-1-*H*-benzotriazole hydrate (HOBt), *N,N*-diisopropylethylamine (DIEA), piperidine, trifluoroacetic acid (TFA), triisopropylsilane (TIS), and *N*<sub>α</sub>-acetyl-L-lysine (Ac-Lys) were purchased from Watanabe Chemical Industries (Hiroshima, Japan). Reagents for Kaiser Test was purchased from Kokusan Chemical Co., Ltd. (Tokyo, Japan). *N,N*-dimethylformamide (DMF) and *N*-ethylmaleimide (NEM) were obtained from Kishida Chemical Co. (Osaka, Japan). Methanol, dichloromethane, diethyl ether, acetonitrile, acetic acid, triethylamine, and Nile red were obtained from Wako Pure Chemical Industries (Osaka, Japan). Fluorescein cadaverine (FC) was purchased from Thermo Fisher Scientific (Waltham, MA, USA). All chemicals and solvents were used as received.

MTG was kindly provided by Ajinomoto Co., Inc. (Tokyo, Japan). Wild-type enhanced green fluorescent protein (wt-EGFP) and EGFP fused with MRHKGS tag (CK-EGFP) were prepared by the previously reported procedure [H. Abe *et al.*, *Chem. Eur. J.* **2011**, *17*, 14004–14008]. The concentrations of WT-EGFP and CR-EGFP were determined using the molar extinction coefficient of 55,000 M<sup>-1</sup>cm<sup>-1</sup> at 488 nm.

**Synthesis of aromatic peptide amphiphiles.** Fmoc-L<sub>n</sub>QG (n = 2, 3) were synthesized by a standard *N*-α-9-fluorenylmethoxycarbonyl (Fmoc) solid-phase peptide synthesis method. In brief, the coupling cycle of each amino acid was done by adding a mixture of coupling reagents (Fmoc-amino acid:HBTU:HOBt:DIEA = 3:3:3:6 mol equivalent to reactive sites on resin) in DMF and the reaction was performed for 1 h at room temperature. After coupling reactions, protective Fmoc group was removed using 20% piperidine in DMF except for the last amino

acid. The aromatic peptides were cleaved from resin using the mixture of 95% TFA, 2.5% TIS, and 2.5% water for 2 h. After the removal of the solvents under reduced pressure, the peptides were precipitated and washed with cold diethyl ether. The crude peptide solids were collected and purified by HPLC on Inertsil ODS-3 column (GL science, Tokyo, Japan) using a gradient of water and acetonitrile both containing 0.1% acetic acid and triethylamine. The fractions with products were collected and lyophilized, and stored at  $-20^{\circ}\text{C}$ . The obtained peptides were analyzed by HPLC (Inertsil ODS-3 column, GL science) and MALDI TOF MS (Autoflex-III, Bruker, Billerica, MA, USA) using  $\alpha$ -cyano-4-hydroxycinnamic acid (CHCA, Sigma-Aldrich) as the matrix.

**Methods.** For the analysis of self-assembly, aromatic peptides were dispersed in 10 mM Tris-HCl buffer (pH 8.0) at the final concentrations of [Fmoc-L<sub>2</sub>QG] = 3.1 mM and [Fmoc-L<sub>3</sub>QG] = 1.7 mM. The solutions were transferred to a micro quartz cell (JASCO Co., Tokyo, Japan) and fluorescence spectra were recorded on a PerkinElmer LS55 with an excitation wavelength of 265 nm at 25 °C. Circular dichroism (CD) spectra were measured by JASCO J-725G using a demountable cuvette with an optical pathlength of 0.1 mm (GL science). For Fourier-transform infrared (FT-IR) spectra, peptide solutions were lyophilized and the resultant solids were used for the analysis on Spectrum Two (PerkinElmer, Waltham, MA, USA). Critical aggregation concentrations were determined by a Nile red encapsulation experiment. Peptide solutions at various concentrations each containing 1  $\mu\text{M}$  Nile red were prepared and incubated overnight at room temperature. The solutions were transferred to a 96 microwell black polystyrene plate (Thermo Scientific) and fluorescence intensities at 635 nm ( $\lambda_{\text{ex}} = 560 \text{ nm}$ ) were recorded on microplate fluorometer (LS-55KG, PerkinElmer). Morphological analysis was performed by transmission electron microscopy (TEM) using a JEM-2010 (JEOL, Tokyo, Japan).

The assembled aromatic peptides ( $[\text{Fmoc-L}_2\text{QG}] = 3.1 \text{ mM}$  and  $[\text{Fmoc-L}_3\text{QG}] = 1.0 \text{ mM}$ ) were drop-cast onto a STEM grid with an elastic carbon film (Okenshoji Co., Tokyo, Japan) and dried. The specimen were stained with 2% uranyl acetate, dried in vacuo, and imaged at an accelerating voltage of 120 kV. Confocal fluorescence images were taken using a Zeiss LSM700 microscope (Carl Zeiss, Oberkochen, Germany) with diode lasers (405 nm for ThT and 488 nm for EGFP).

## 2. Characterization of Fmoc-LnQG peptides

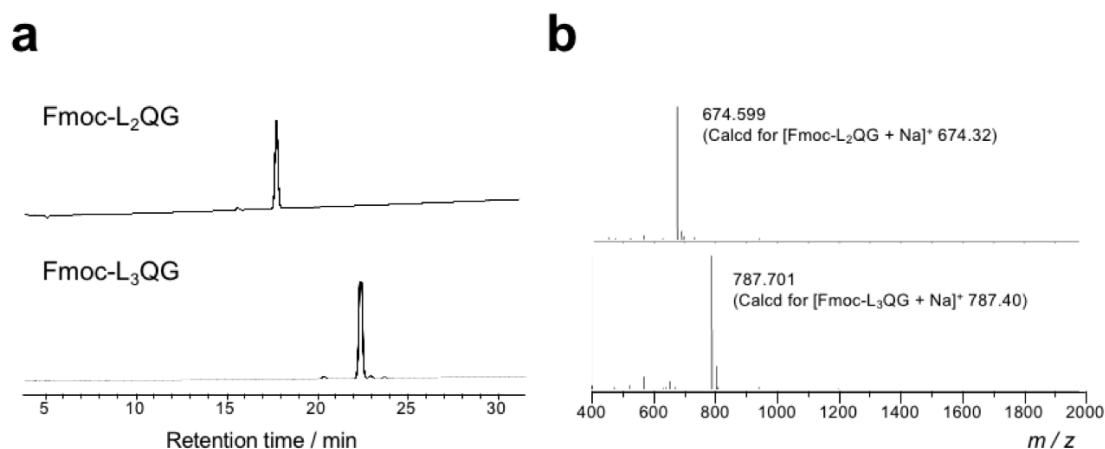


**Fig. S1** Characterization of Fmoc-L<sub>2</sub>QG (top) and Fmoc-L<sub>3</sub>QG (bottom) by HPLC (a) and MALDI TOF MS (b). Conditions: (a) Inertsil ODS-3 (GL science, 4.6×250 mm), 40%B to 70%B in 30 min (A: water, B: acetonitrile, both containing 0.1% TFA), 1 mL/min, 220 nm detection. (b) reflector positive mode using  $\alpha$ -CHCA as a matrix.

## 3. Critical aggregation concentration determination of Fmoc-LnQG peptides

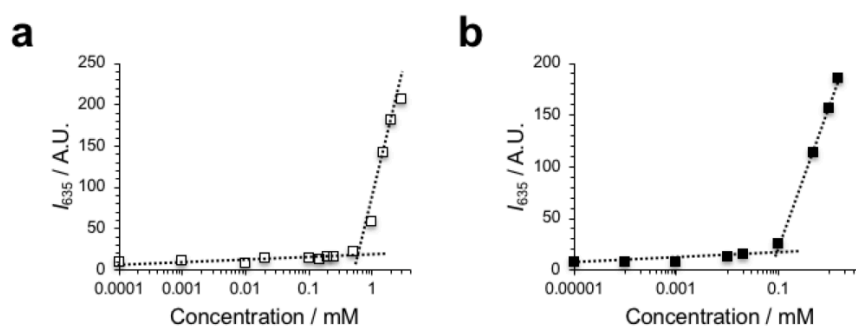


**Fig. S2** Critical aggregation concentration determination of Fmoc-L<sub>2</sub>QG (a) and Fmoc-L<sub>3</sub>QG (b) using Nile red at the final concentration of 1  $\mu$ M.  $\lambda_{\text{ex}} = 560$  nm.

#### 4. Confocal fluorescence microscope images of Fmoc-LnQG peptide assemblies

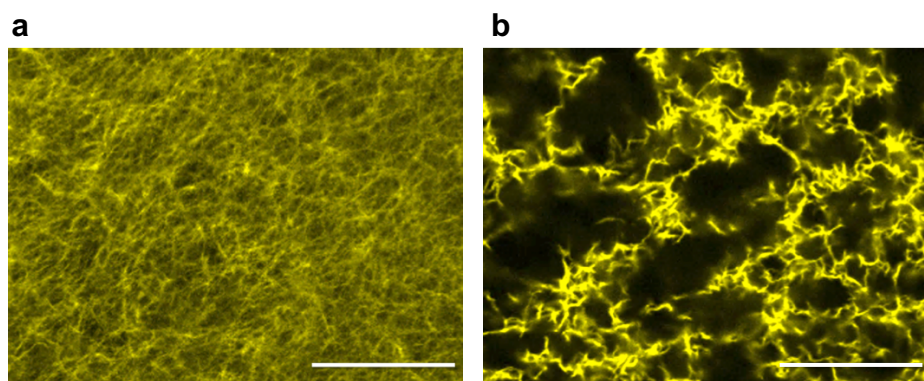


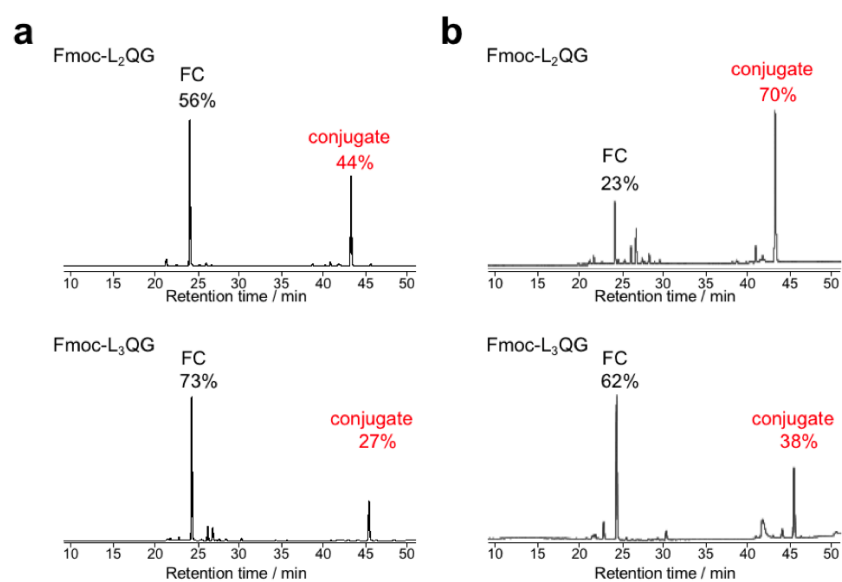
**Fig. S3** Confocal fluorescence images of Fmoc-L<sub>2</sub>QG (a) and Fmoc-L<sub>3</sub>QG (b). Peptide assemblies were stained with 10  $\mu$ M Thioflavin T. Bars: 20  $\mu$ m.

#### 5. Conjugation of Fmoc-LnQG and fluorescein cadaverine (FC) by MTG catalysis

The reaction mixtures of Fmoc-LnQG and fluorescein cadaverine (FC) were prepared ([Fmoc-L<sub>2</sub>QG] = 2.0 mM, [Fmoc-L<sub>3</sub>QG] = 1.0 mM, FC:Fmoc-LnQG = 1:100 or 1:10 molar ratio) in 10 mM Tris-HCl buffer (pH 8.0), then MTG (0.3 U/mL) was added to the mixtures. After the reaction proceeded at 25 °C for 2 h, NEM was added at the final concentration of 1 mM to terminate the reaction. MALDI TOF MS was measured with a Bruker Autoflex-III using  $\alpha$ -cyano-4-hydroxycinnamic acid (CHCA, Sigma-Aldrich) as the matrix (Table S1). Conjugation rates were analyzed by HPLC using an Inertsil ODS-3 column with the flow rate at 1 mL/min and the detection wavelength at 438 nm (Fig. S4).

**Table S1.** MALDI TOF MF analysis of MTG reaction of Fmoc-LnQG and FC.

peptides	MTG reaction	$[M+H]^+_{\text{obs}}$	$[M+H]^+_{\text{calc}}$	$[M+Na]^+_{\text{obs}}$	$[M+Na]^+_{\text{calc}}$
Fmoc-L <sub>2</sub> QG	+	1126.43	1126.45	—	1148.44
	-	—	652.33	674.27	674.32
Fmoc-L <sub>3</sub> QG	+	1239.89	1239.54	—	1261.53
	-	—	765.41	787.60	787.40

**Fig. S4** HPLC analysis of MTG-catalyzed conjugation of FC and Fmoc-LnQG at molar ratio of FC:Fmoc-LnQG = 1:10 (a) or 1:100 (b). HPLC conditions: Inertsil ODS-3 (GL science, 4.6 × 250 mm), 2%B to 80%B in 50 min (A: water, B: acetonitrile, both containing 0.1% TFA), 1 mL/min, 436 nm detection.

## 6. Confocal fluorescence microscope images of FC on Fmoc-LnQG peptide assemblies

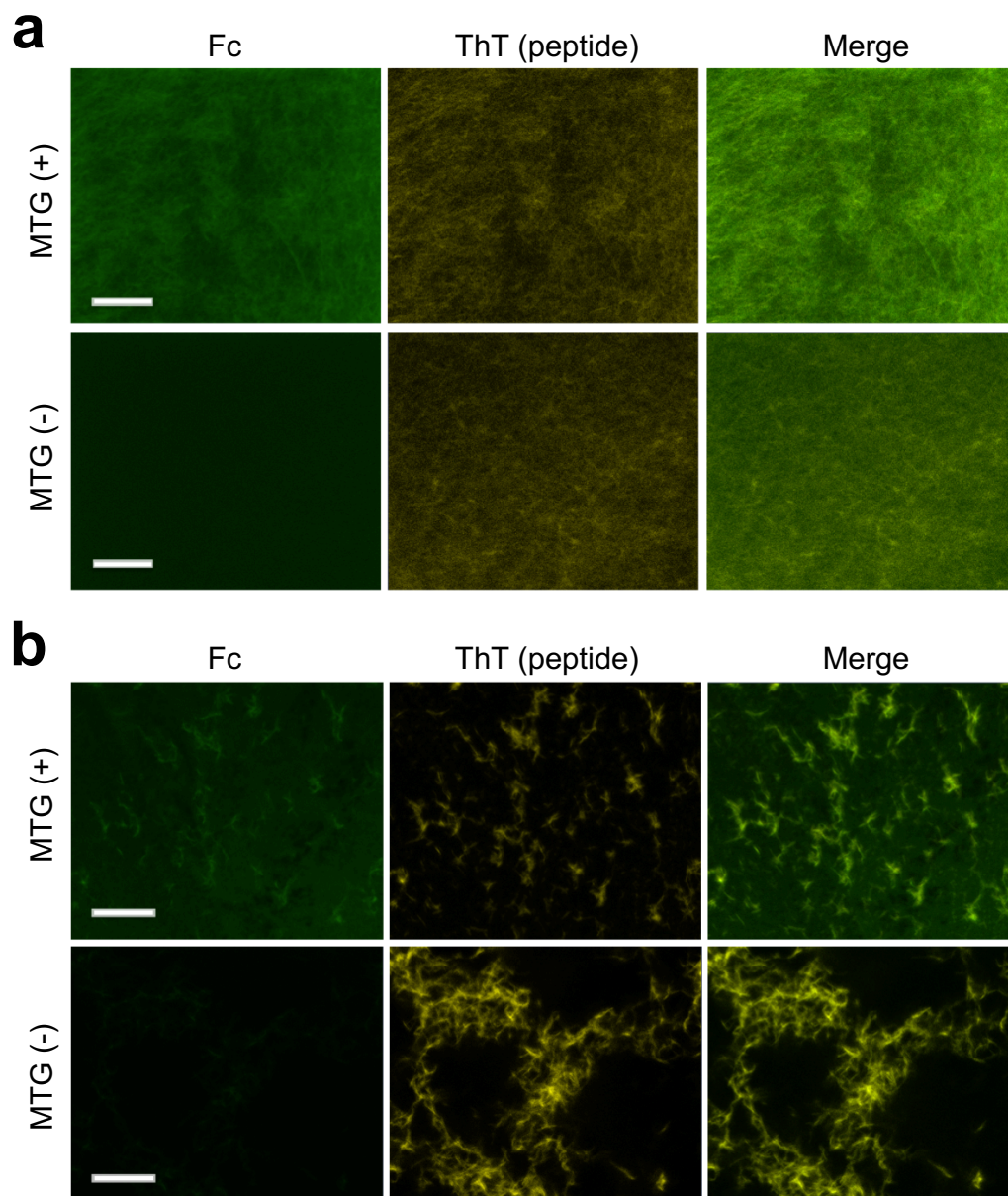


**Fig. S5** FC assembly on the structures of Fmoc-L<sub>2</sub>QG (a) and Fmoc-L<sub>3</sub>QG (b). Peptide assemblies were stained with 10  $\mu$ M Thioflavin T. Bars: 10  $\mu$ m.



## 7. Reaction kinetics of MTG-catalyzed reaction of Fmoc-LnQG

Various concentrations of Fmoc-LnQG were prepared using 10 mM Tris-HCl buffer (pH 8.0). Ac-Lys (20 mM) and MTG (0.2 U/mL) were added, and MTG reaction was proceeded at 25°C. At intervals, aliquots of the reaction mixture were withdrawn and the reaction was terminated by adding NEM. The production of conjugation was analyzed by HPLC using an Inertsil ODS-3 column with the flow rate at 1 mL/min and the detection wavelength at 260 nm, where free Fmoc-L<sub>2</sub>QG and Fmoc-L<sub>3</sub>QG were detected at 16.1 and 20.4 min, respectively, while conjugates for those were at 14.5 and 18.3 min, respectively (Fig. S6).

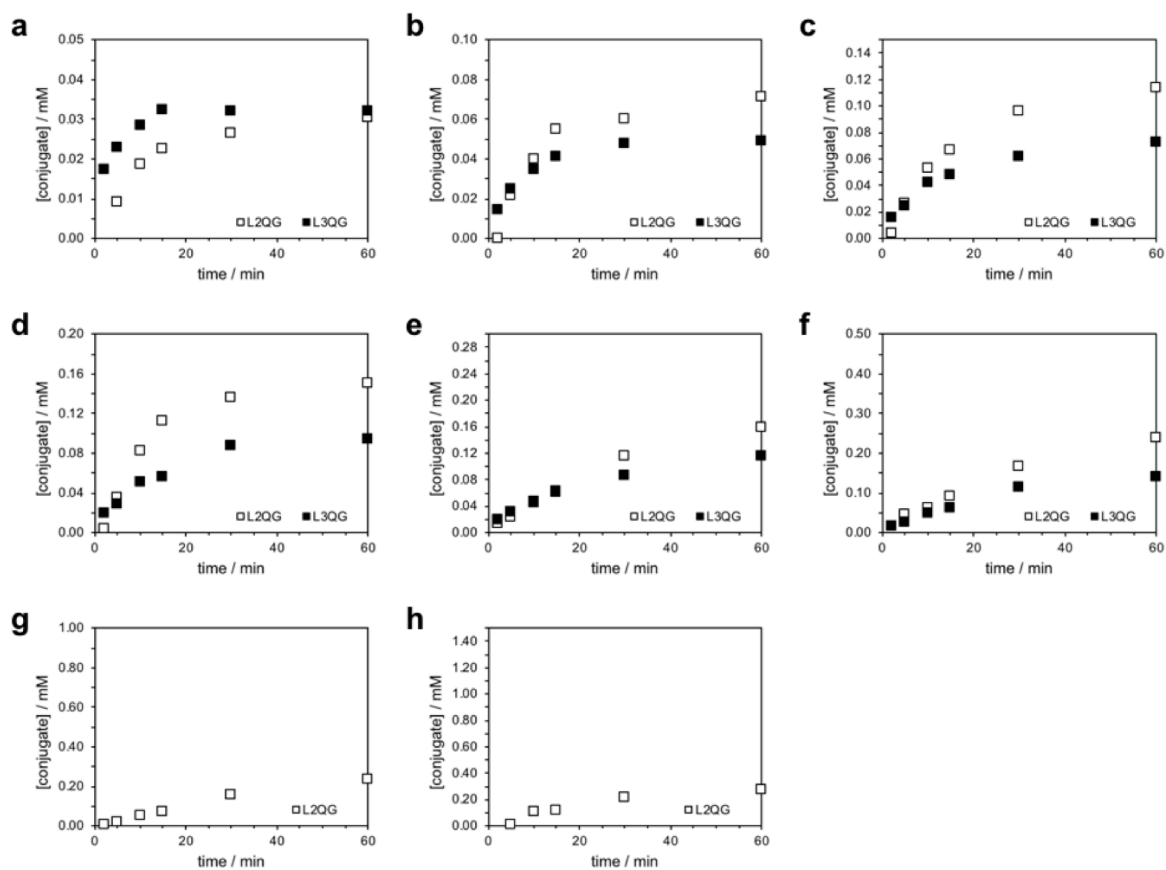


**Fig. S6** Reaction rates of Fmoc-LnQG at [Fmoc-LnQG] = (a) 50, (b) 100, (c) 150, (d) 200, (e) 300, (f) 500, (g) 1000, (h) 1500  $\mu\text{M}$  by MTG. HPLC conditions: Inertsil ODS-3 (GL science, 4.6  $\times$  250 mm), 40%B to 70%B in 30 min (A: water, B: acetonitrile, both containing 0.1% TFA), 1 mL/min, 260 nm detection.

## 8. Difference in the reaction kinetics by MTG between Fmoc-L<sub>2</sub>QG and Fmoc-L<sub>3</sub>QG

The initial velocities of each experimental condition were calculated by the slopes in the linear region at the beginning of the reaction (2–10 or 15 min) in Fig. S6 and were plotted against Fmoc-LnQG concentrations.

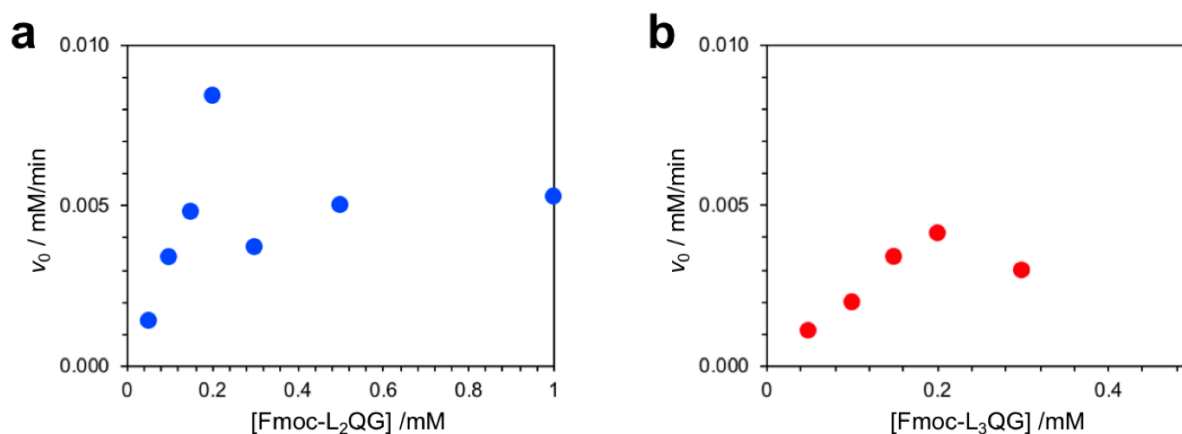


**Fig. S7** Plots of initial velocities of MTG reaction against Fmoc-L<sub>2</sub>QG (a) and Fmoc-L<sub>3</sub>QG (b) concentrations.

## 9. Sequence of proteins used in this study

**Table S2.** N- and C-terminal amino acid sequences of EGFP used in this study.

Protein	Amino acid sequence of N- and C-terminal regions
WT-EGFP ( $\Delta K_{238}$ )	<b>MHHHHHHMVSKG-----DELY</b> (237 residues)
CK-EGFP	<b>MHHHHHHMVSKG-----DELYRMRH<u>K</u>GS</b> (244 residues)

## 10. Time-course of conjugation of Fmoc-L<sub>2</sub>QG with CK-EGFP by MTG

Fmoc-L<sub>2</sub>QG or Fmoc-L<sub>3</sub>QG was dispersed in 10 mM Tris-HCl buffer ([Fmoc-L<sub>2</sub>QG] = 2.0 mM, [Fmoc-L<sub>3</sub>QG] = 1.0 mM), and CK-EGFP (10 μM) and MTG (0.3 U/mL) were added. The reaction was proceeded at 25°C. At intervals, aliquots of the reaction mixture were withdrawn and the reaction was terminated by adding NEM. The production of the conjugates was analyzed by HPLC using an Inertsil ODS-3 column with the flow rate at 1 mL/min and the detection wavelength at 280 nm, where free CK-EGFP and the conjugate with Fmoc-LnQG were detected at 12.8 and 14.9 min, respectively (Fig. S4).

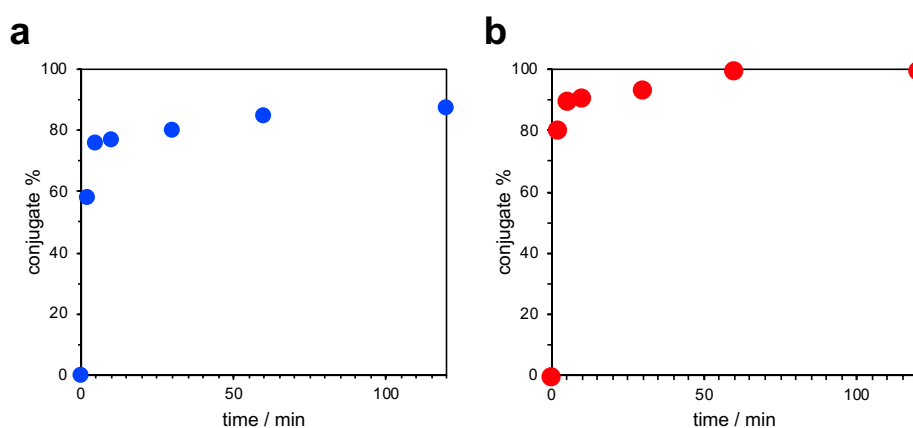


**Fig. S8** (a) Conjugation of CK-EGFP on Fmoc-L<sub>2</sub>QG (a) and Fmoc-L<sub>3</sub>QG (b). [Fmoc-L<sub>2</sub>QG] = 2.0 mM, [Fmoc-L<sub>3</sub>QG] = 1.0 mM, [CK-EGFP] = 10 μM, [MTG] = 0.3 U/mL, 25°C. HPLC conditions: Inertsil ODS-3 (GL science, 4.6 × 250 mm), 20%B to 80%B in 30 min (A: water, B: acetonitrile, both containing 0.1% TFA), 1 mL/min, 280 nm detection.

## 11. Fluorescence properties of CK-EGFP before and after MTG reaction

After the MTG reaction in Fig. S7, the reaction mixture was diluted 100-fold (final concentration of CK-EGFP = 0.1  $\mu$ M) using 10 mM HCl buffer (pH 8.0). As a control, CK-EGFP without MTG reaction was prepared at the same concentration. Fluorescence spectra were recorded on PerkinElmer LS55 with an excitation wavelength of 488 nm at 25  $^{\circ}$ C.

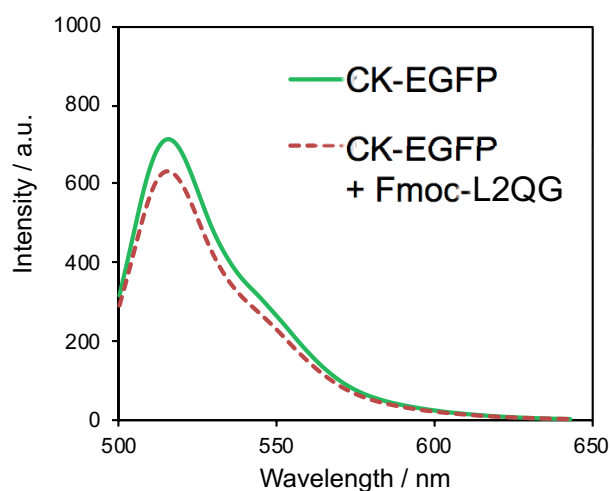


**Fig. S9** Fluorescence spectra of CK-EGFP before and after MTG reaction.  $\lambda_{\text{ex}} = 488$  nm.

## 12. Influence of MTG reaction on Fmoc-LnQG peptide assemblies

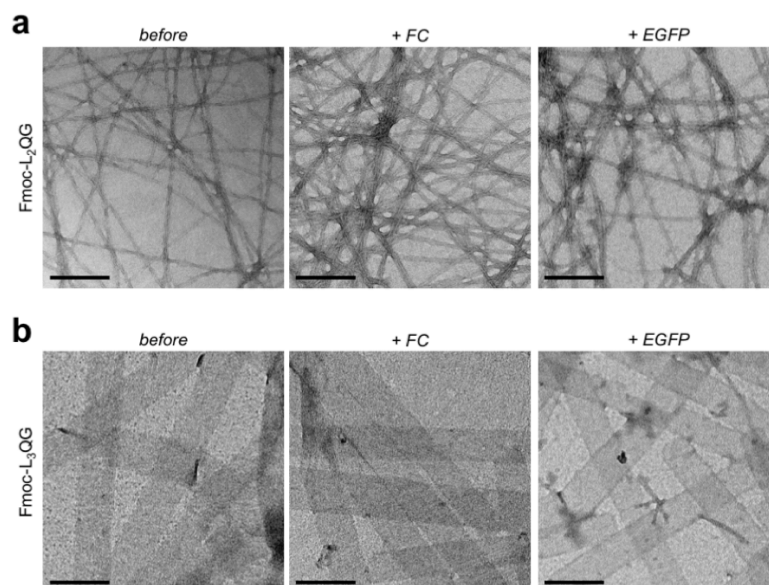


**Fig. S10** TEM images of Fmoc-L<sub>2</sub>QG (a) and Fmoc-L<sub>3</sub>QG (b) before and after the MTG reaction. (a) [Fmoc-L<sub>2</sub>QG] = 2.0 mM, [FC] = 20  $\mu$ M or [CRK-EGFP] = 10  $\mu$ M, [MTG] = 0.3 U/mL in 10 mM Tris-HCl (pH 8.0), 25°C, 2 h; (b) [Fmoc-L<sub>3</sub>QG] = 1.0 mM, [FC] = 10  $\mu$ M or [CRK-EGFP] = 10  $\mu$ M, [MTG] = 0.3 U/mL in 10 mM Tris-HCl (pH 8.0), 25°C, 2 h. Bars: 200 nm.

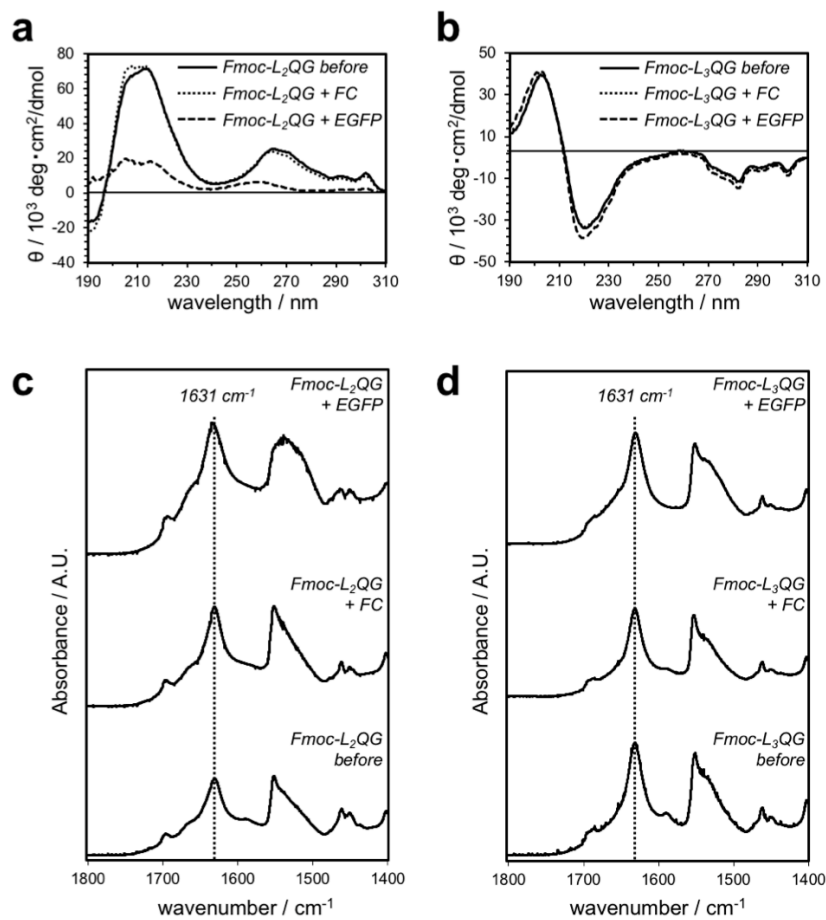


**Fig. S11** Influence of MTG reaction on the self-assembly structures of Fmoc-L<sub>n</sub>QG. (a, b) CD spectra of Fmoc-L<sub>2</sub>QG (a) and Fmoc-L<sub>3</sub>QG (b); (c, d) FT-IR spectra of Fmoc-L<sub>2</sub>QG (c) and Fmoc-L<sub>3</sub>QG (d).

### 13. Influence of MTG reaction on CK-EGFP display on Fmoc-LnQG peptide assemblies

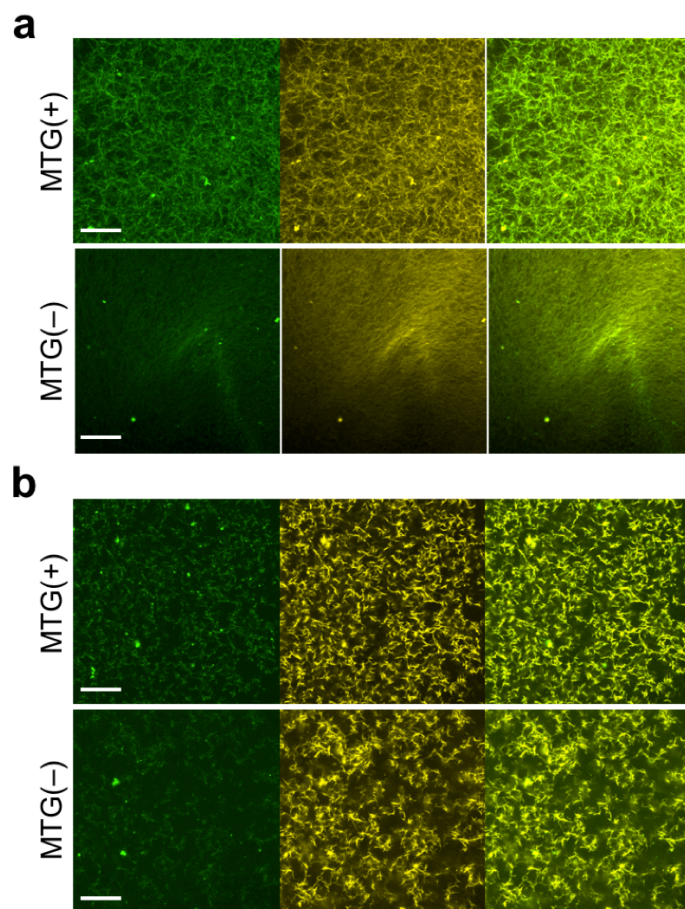


**Fig. S12** Enzymatic display of CK-EGFP on Fmoc-L<sub>2</sub>QG (a) and Fmoc-L<sub>3</sub>QG (b) assembly. Peptide assemblies were stained with 100  $\mu$ M Thioflavin T. Bars: 20  $\mu$ m.

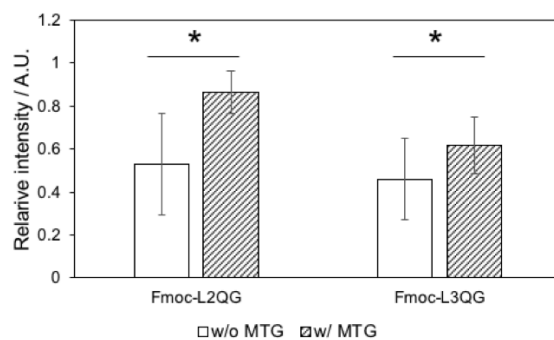


**Fig. S13** Influence of MTG reaction on CK-EGFP display on Fmoc-L<sub>2</sub>QG. Fluorescence intensities from CK-EGFP were normalized using those from Thioflavin T to eliminate the influence of image location. For each condition, randomly taken 5–10 images were analyzed. \* $p < 0.05$ .

#### 14. Conjugation of CK-EGFP on Fmoc-LnQG by MTG catalysis

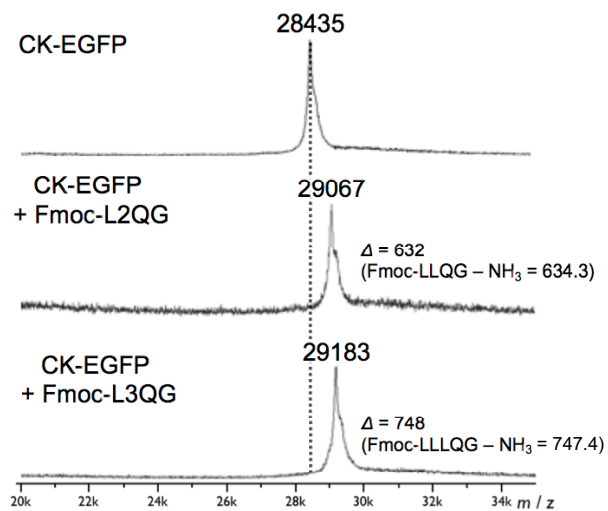


**Fig. S14** MALDI TOF MS analysis of MTG-catalyzed conjugation of CK-EGFP and Fmoc-LnQG. Linear positive mode, matrix: CHCA.